WARSAW UNIVERSITY OF TECHNOLOGY Index 351733
FACULTY OF CIVIL ENGINEERING
COMMITTEE FOR CIVIL AND WATER ENGINEERING
POLISH ACADEMY OF SCIENCES ISSN 1230-2945
DOI: 10.24425/ace.2024.151915
ARCHIVES OF CIVIL ENGINEERING
Vol. LXX ISSUE 4 2024
pp. 649–666

Research paper

Construction monitoring and control of cable-stayed bridges without backstays

Xilong Zheng[1]

Abstract: The cable-stayed bridge without backstays is an important branch of the cable-stayed bridge family. It tilts the bridge tower to one side and removes the backstay, using its own weight to balance the cable tension. It has the characteristics of novel structure and beautiful appearance and is highly favoured in urban construction both at home and abroad. In this paper, based on the construction of the main bridge of Jinzhou Bridge, a spatial model was established using finite element analysis software to simulate and analyse the construction process, with a focus on researching the construction control. Jinzhou Bridge has a novel structure and complex technology. The inclination angle of the bridge tower is the largest among its counterparts, and the difficulty of construction control is relatively high. This paper uses the adaptive control theory to control the construction of the main bridge of Jinzhou Bridge. During the construction process and the bridge state, the structure of Jinzhou Bridge is subject to reasonable stress and the bridge body is safe and reliable. The line shape of the main beam is basically smooth, further demonstrating the correctness of the construction control theory data.

Keywords: cable-stayed bridges without backstays, construction monitoring and control, finite element simulation, construction methods

[1]PhD., Harbin University, School of Civil and Architectural Engineering, No.109 Zhongxing Da Dao, Harbin, China, e-mail: sampson88@126.com, ORCID: 0000-0001-5571-667X

1. Introduction

Cable-stayed bridges are a type of bridge in which the bridge deck system is under compression and the supporting system is under tension. The bridge deck system is composed of a stiffening beam, while the supporting system is made up of steel cables [1]. Its main feature is the use of diagonal cables as elastic supports for the beam span, reducing the bending moment of the cross-section of the beam span, reducing the weight of the main beam, and enhancing the bridge's crossing capacity [2–4].

Since the 1990s, with the development of cable-stayed bridge construction technology worldwide, China's cable-stayed bridges have encountered new development opportunities. Many large-span cable-stayed bridges with spans exceeding 500 m have been successively built, including the representative bridges of Shanghai Nanpu Bridge and Yangpu Bridge [5]. These construction projects have cultivated numerous talents in bridge design and construction and accumulated a wealth of valuable construction experience and technology. Later, a group of cable-stayed bridges with world-leading levels and spans of up to one kilometer were built. Through decades of hard work and independent innovation, China's cable-stayed bridge construction level is advancing towards the world's top level [6–8].

Cable-stayed bridges without backstays have a strong visual impact, which is enough to attract people's attention. Once constructed, they become iconic structures representing the city and are favoured by designers and local governments [9–11]. However, this bridge type is not widely constructed worldwide, and the analysis shows several reasons for this. Firstly, the cable-stayed bridge without backstays has a complex stress state and requires consideration of multiple factors, which limits the extent of related design work. Secondly, due to the unique structural form of this bridge type, the construction difficulties are greater compared to conventional cable-stayed bridges with the same span [12].

Due to the inclined position of the bridge towers of cable-stayed bridges without backstays, the construction methods used differ slightly from those of conventional cable-stayed bridges. The commonly used construction method is tower-beam synchronous construction, in which the construction of the tower and beam overlap and the cable hanging and tensioning work can be carried out at the same time [13]. By adopting this method, construction support facilities for inclined bridge towers can be eliminated, construction area can be reduced, and the construction period and cost can be shortened. This method has been validated in the construction of several cable-stayed bridges [14, 15].

Compared with conventional cable-stayed bridges, cable-stayed bridges without backstays have greater construction difficulty and require more complex technology. Therefore, controlling the construction process is more essential and challenging, as more parameters need to be controlled and analyzed. This article relies on the main bridge construction of the Jinzhou Bridge, which has a novel structure, complex technology, and the highest tower inclination angle among similar bridges. It introduces the basic situation and control effect of the main bridge construction control of the Jinzhou Bridge.

2. Engineering background

The main bridge of Jinzhou Bridge in Dalian, Liaoning Province, is a single-tower, single-cable-surface cable-stayed bridge with a fixed system of piers, towers, and beams. The maximum longitudinal slope of the bridge deck is 1.38%, and the main span is on a convex vertical curve with a radius of 14,000 m. The cable tower adopts drilled pile foundation and a single-column inclined steel-reinforced concrete tower with a variable rectangular cross-section. The height of the cable tower is 124.2 m.

The main beam adopts a steel-concrete composite box girder with a concrete bridge deck on its top. The beam has a height of 3.0 m at the centerline and a full width of 30.5 m. The bridge deck has a 2% bidirectional cross slope. The inclined tension cables use finished parallel steel wires with a PE protective cover. The elevation of the Jinzhou Bridge main bridge is shown in Fig. 1.

Fig. 1. Elevation drawing of the main bridge of Jinzhou bridge

1. Cable tower

The cable tower adopts a single-column concrete inclined tower with a horizontal inclination angle of 55°and a rearward inclination angle of 35°. The rearward inclination angle of the tower is the largest among similar types of bridges. The total height of the cable tower is 124.2 m.

2. Main beam

The main beam of this bridge is divided into concrete box girder and steel-concrete composite box girder. The concrete box girder is the main beam at the junction of pier, tower, and beam, with a length of 10.0 m and a central beam height of 3.0 m, as shown in Fig. 2. The steel-concrete composite box girder has a central beam height of 3 m. The top slab of the box

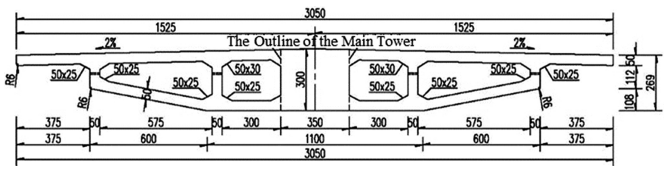

Fig. 2. Cross-sectional diagram of the main bridge of Jinzhou Bridge (1) (mm)

girder is made of C50 polypropylene fiber concrete, while the bottom slab and web plates are made of steel. The steel-concrete composite beam has a top width of 30.5 m, a bottom width of 10.0 m, and the cross-section is shown in Fig. 3 and Fig. 4.

The steel box girder is equipped with transverse partitions and longitudinal stiffeners. The bottom plate of the steel box girder is 24 thick, the wing plate is 20 thick, the inner web plate is 30 thick, and the transverse partition is 20 thick.

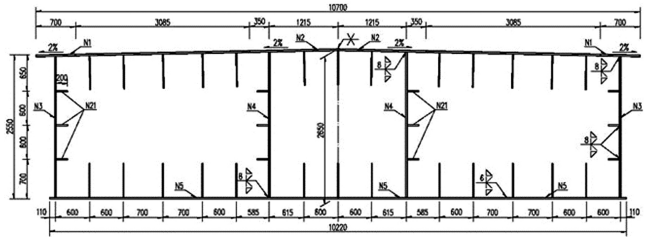

Fig. 3. Cross-sectional diagram of the main bridge of Jinzhou Bridge (2) (mm)

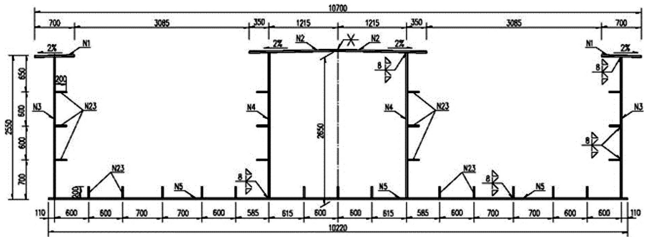

Fig. 4. Cross-sectional diagram of the main bridge of Jinzhou Bridge (3) (mm)

3. Cable tower

The cables are arranged in a harp shape, with a horizontal spacing of 1.6 m between cable anchoring points on the beam. The standard cable spacing for diagonal cables on the main beam is 12.0 m, and the first pair of cables extend to 22.0 m at the tower intersection. There are three types of cables, with 6 of each type, for a total of 18 cables. The longest cable is 196.055 m, and the shortest is 44.732 m. Fixed-end anchorages are used at the cable towers, and tensioning-end anchorages are used within the main beam.

3. Simulation calculation of the construction process

3.1. Construction methods and steps

The construction of the main bridge of Jinzhou Bridge is a complex system engineering. According to different construction sites and methods, it is mainly divided into pier cap construction, bridge tower construction, main beam construction, and cable tensioning.

The construction of the bridge tower is divided from bottom to top into three main sections: section C with a double-chamber box-shaped tower pier section, section B with a rectangular solid section tower pier beam rigid connection transition, and section A with a large inclination H-shaped cable section based on the section changes and structural characteristics of the cable tower structure. Sections C and B adopt the segmental turnover formwork construction method with a scaffolding support system, while Section A adopts the climbing formwork construction method. Regardless of the changes in the appearance of the tower column, the pouring segments are all horizontally divided. The segment division of the cable tower construction is shown in Fig. 5.

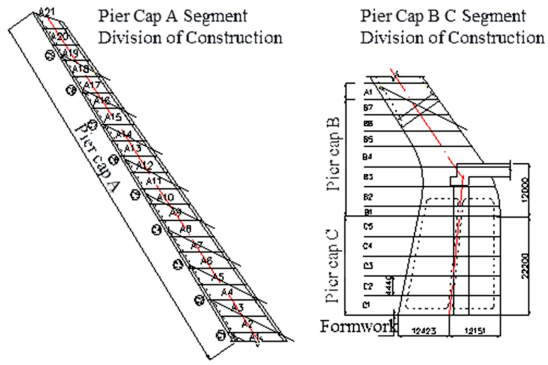

Fig. 5. Diagram of segmented construction for cable-stayed towers (mm)

The main beam of the entire bridge is divided into 22 construction segments, as shown in Fig. 6. They are respectively the cast-in-place concrete segment S1, the steel-concrete composite segment S2, the steel spliced segments S3 and S22, and the steel-concrete hybrid standard segments S4 to S21.

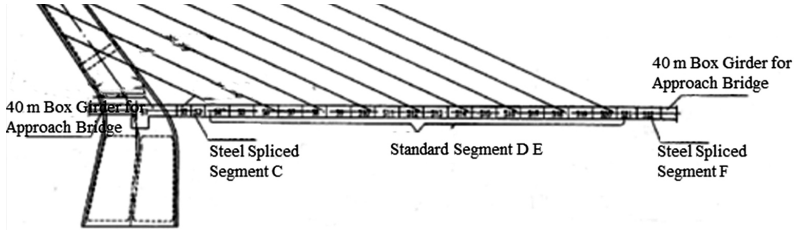

Fig. 6. Diagram of main girder construction segment division

3.2. Major calculation parameters

The structural parameters taken in finite element analysis are mainly based on the construction drawings provided by the design party and the regulations of relevant national standards. During the construction process of a bridge, these parameters may undergo changes,

and their values need to conform to the actual conditions, which are adjusted continuously with the help of on-site testing data.

The pylon of the cable-stayed tower, as well as the main concrete girder of the main bridge, adopts C50 concrete with an elastic modulus of 3.45×10^4 MPa. The axial compressive design strength is 22.4 MPa, and the axial tensile design strength is 1.83 MPa. The linear expansion coefficient is 10^{-5}. The steel plates of the steel box girder are made of Q345qE steel grade, and all properties meet the requirements of GB/T714-2000. The high-strength bolts used for connections comply with GB1228-2006. The steel strands of the stay cables are coated with epoxy, with a tensile strength (f_{pk}) of 1860 MPa and an elastic modulus (E) of $(1.9 \pm 0.1) \times 10^5$ MPa. The elastic modulus of prestressed steel reinforcement in the concrete box girder is 1.95×10^5 MPa.

3.3. Structural analysis model establishment

(1) Discretization of the structure

The modeling and analysis of the main bridge of Jinzhou Bridge are performed using the Midas/Civil finite element analysis software. A spatial truss system model is established. According to the calculation method of finite element analysis, before building the model, the structure needs to be discretized. The division of the entire bridge units is shown in Fig. 7.

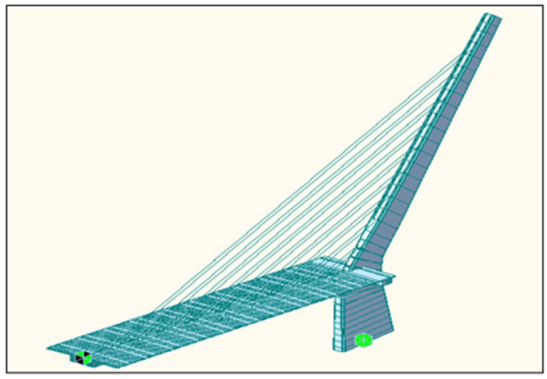

Fig. 7. Finite element discretization diagram of the structure

When simulating the main beam, the stiffness (torsional stiffness, lateral bending stiffness, and vertical bending stiffness) and mass of the main beam are all concentrated on the central axis of the main beam. The constraints on the main beam at the pier are modeled using general supports that constrain the horizontal lateral displacement Dy, vertical displacement Dz, and rotation around the z-axis Rz, based on the actual types of supports set.

(2) Construction stage setup

With the help of Midas/Civil's construction process simulation function, a total of 41 construction stages have been established in conjunction with the construction steps, as shown in Table 1.

Table 1. Construction stage division table

Construction stages	**Construction activities**	**Construction duration (day)**	**Construction phases**	**Construction scope**	**Construction duration (day)**
1	Tower pier construction	180	22	Construction of the main beam of the C7 section of the cable-stayed bridge	10
2	Construction of the cast-in-place segment of the main beam	50	23	First tensioning of the cable-stay in the C7 section	1
3	Construction of the main tower of the C2 section of the cable-stayed bridge	10	24	Construction of the main beam of the C9 section of the cable-stayed bridge	10
4	Construction of the main tower of the C1 section of the cable-stayed bridge	10	25	Construction of the main beam of the C8 section of the cable-stayed bridge	10
5	First tensioning of the cable-stay in the C1 section	1	26	First tensioning of the cable-stay in the C8 section	1
6	The construction of the main tower for the C3 section of the cable-stay is underway	10	27	The construction of the main beam for the C9 section of the cable-stay is underway	10
7	The construction of the main beam for the C2 section of the cable-stay is underway	10	28	First tensioning of the cable-stay in the C9 section	1
8	First tensioning of the cable-stay in the C2 section	1	29	The remaining sections of the main beam are currently under construction	10
9	The construction of the main tower for the C4 section of the cable-stay is underway	10	30	The dismantling of the support structure is in progress	1
10	The construction of the main beam for the C3 section of the cable-stay is currently underway	10	31	The second tensioning of the C9 cable-stay	1
11	The first tensioning of the C3 cable-stay.	1	32	The second tensioning of the C8 cable-stay.	1

Table 1. [cont.]

Construction stages	Construction activities	Construction duration (day)	Construction phases	Construction scope	Construction duration (day)
12	The main tower construction for the C5 cable-stay section is currently underway	10	33	The second tensioning of the C7 cable-stay	1
13	The main beam construction for the C4 cable-stay section is in progress	10	34	The second tensioning of the C6 cable-stay.	1
14	The first tensioning of the C4 cable-stay	1	35	The second tensioning of the C5 cable-stay	1
15	The construction of the main tower for the C6 cable-stay section	10	36	The second tensioning of the C4 cable-stay	1
16	The construction of the main tower for the C5 cable-stay section	10	37	The second tensioning of the C3 cable-stay	1
17	The first tensioning of the C5 cable-stay	1	38	The second tensioning of the C2 cable-stay	1
18	The construction of the main tower for the C7 cable-stay section	10	39	The second tensioning of the C1 cable-stay	1
19	The construction of the main tower for the C6 cable-stay section	10	40	Bridge deck paving and other construction works	30
20	The first tensioning of the C6 cable-stay	1	41	Ten years of bridge operation	3650
21	The construction of the main tower for the C8 cable-stay section	10			

From the above table, it can be seen that during construction stages 3 to 28, there is mainly a repetitive construction process, with each cycle consisting of three construction activities (taking the second cycle as an example): pouring of the corresponding main tower segment for cable-stayed span C3, construction of the corresponding main beam segment for cable-stayed span C2, and tensioning of cable-stayed span C2.

4. Control and monitoring during the construction process

4.1. Monitoring of structural stress and structural temperature field

The main stress monitoring of Jinzhou Bridge focuses on measuring the stress changes of several control sections of the main beam and bridge towers before and after certain working conditions. Based on the continuous monitoring of stress, the loading condition of the main beam can be determined to ensure compliance with safety requirements and to maintain a safe construction environment. This observation is conducted at each construction stage.

The stress monitoring sections for the main beam and bridge towers are selected at the construction and installation stages, as well as during the completion stage when extreme stress values occur. A total of nine sections are selected, including the main beam sections at the tower-beam junction, the steel-box beam and concrete junction, the front sections of assembly segments S7, S12, and S18 of the main beam. The tower sections include the upper and lower sections at the tower-beam junction, the section near the C1 cable anchor point, and the section near the C4 cable anchor point. The specific arrangement of monitoring sections is shown in Fig. 8.

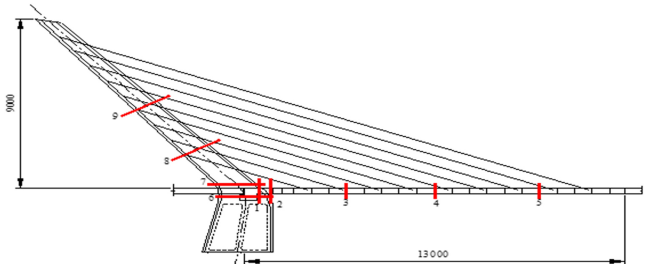

Fig. 8. Layout diagram for stress and temperature monitoring sections (cm)

In the stress measurement of the main bridge of Jinzhou Bridge, strain sensors are embedded in the monitoring sections to indirectly measure the stress values based on the section strains. To ensure more accurate measurement results, surface-mounted FRP-encased fiber optic grating strain sensors are chosen for strain monitoring of the steel structure. For the strain monitoring of the prestressed reinforced concrete structure at the junction of the beam and tower, highly durable end-bulge CFRP-encased fiber optic grating strain sensors are used.

There are 10 strain sensors and 4 temperature sensors arranged at various control sections of the concrete beam segments. The strain sensors are fixed on the longitudinal main reinforcement, while the temperature sensors are tied to the main reinforcement with fine wire. The testing wires are led outside the box and properly labeled and protected. The layout of the sensors is shown in Fig. 9.

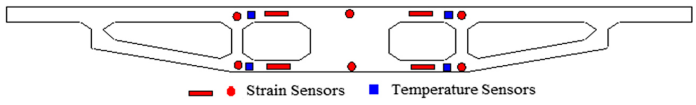

Fig. 9. Layout diagram of sensors within section 1 and section 2

The control section at the steel-concrete junction is equipped with 12 strain sensors and 4 temperature sensors. The strain and temperature sensors are fixed on the top and bottom plates of the steel box beam respectively. The testing wires are led out of the box and properly labeled and protected. The layout of the sensors is shown in Fig. 10.

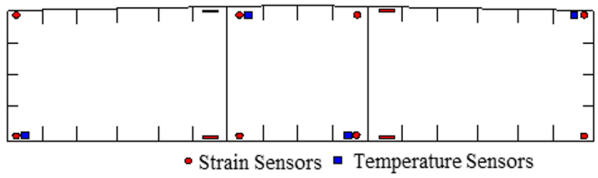

Fig. 10. Layout diagram of sensors within section 3 and section 5

Each control section of the steel box girder segment is equipped with 8 strain sensors and 8 temperature sensors. The strain and temperature sensors are fixed on the top and bottom plates of the steel box girder respectively. The testing wires are led out of the box and properly labeled and protected. The layout of the sensors is shown in Fig. 11.

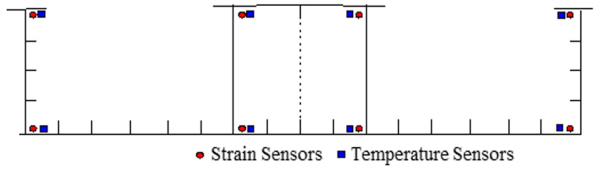

Fig. 11. Layout diagram of sensors within section 4

Each control section of the bridge tower is equipped with 4 strain sensors and 2 temperature sensors. The 2 temperature sensors are positioned at the diagonal corners of the bridge tower section. The layout of the sensors is shown in Fig. 12 and Fig. 13.

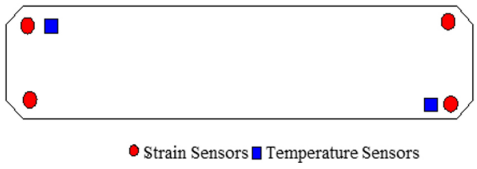

Fig. 12. Layout diagram of sensors within section 6

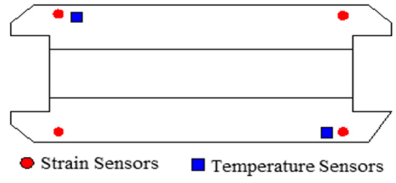

Fig. 13. Layout diagram of sensors within section 7, 8, 9

The on-site sensor arrangement and testing situation are shown in Fig. 14 and Fig. 15.

Fig. 14. Strain sensor installation diagram

Fig. 15. On-site strain testing diagram

4.2. Structural alignment monitoring

4.2.1. Monitoring of main tower displacement and main tower foundation settlement

The measurement of main tower displacement includes the measurement of displacement values in both longitudinal and transverse directions. The Leica TCA2003 total station is primarily used for measurements. By using the coordinate method, the displacement values of the tower are calculated based on the difference between two measurements of pre-set measurement points located at the top and middle of the tower. Continuous measurements are carried out for 24 hours under typical weather and natural conditions, and additional measurements are taken after each completion of cable tensioning.

4.2.2. Monitoring of main girder elevation and alignment deviation

During the monitoring, the elevation of the main girder measurement points is obtained by referencing the benchmark points on the tower column using Leica's NA2 precision level. There are 5 measurement points arranged for each girder section, including: 1 point at the centerline of the main girder, 2 points symmetrically arranged at the center of the bridge deck wet joints on the two flanges of the steel box girder, and 2 points symmetrically arranged on the edges of the bridge deck on both sides. The specific arrangement of the measurement points is shown in Fig. 16.

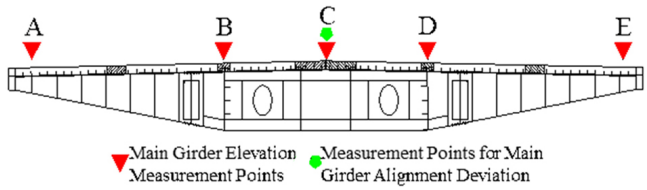

Fig. 16. Layout plan for main girder elevation and alignment deviation measurement

The measurement of the main girder alignment deviation mainly takes place during each girder section installation or after the tensioning of the stay cables. It involves measuring the alignment deviation of the front 5 girder sections and making adjustments to the cable forces, as well as measuring partial or full bridge alignment before and after the closure and pouring of the bridge deck. The measurement method involves using the Leica TCA2003 total station. The total station is used to measure its planar coordinates, which are then compared with the design values to determine the actual deviation value. The measurement positioning points and measurement drawings for the main girder on-site are shown in Fig. 17 and Fig. 18.

Fig. 17. Positioning points for main girder elevation measurement

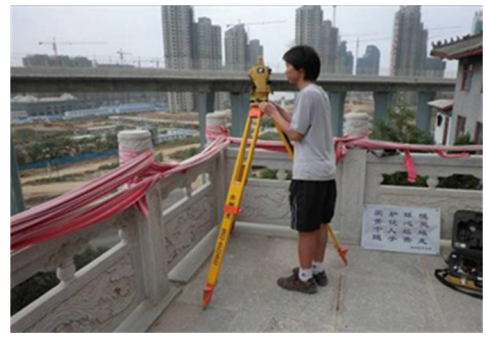

Fig. 18. On-site elevation measurement diagram

4.3. Cable force monitoring

The main bridge of Jinzhou Bridge adopts the frequency method for cable force measurement, which utilizes the corresponding relationship between cable force and the vibration frequency of the cable. By measuring the vibration frequency of the cable and using string theory calculations, the tension of the cable can be determined. During on-site measurements, specially designed straps are used to vertically attach accelerometers to the cables. Artificial excitation is applied, and the cable force dynamometer is used for recording and spectral analysis.

5. Construction control effectiveness of the main bridge of Jinzhou bridge

5.1. Key construction phase control effectiveness

Construction control is implemented throughout the entire construction process. In order to achieve construction control over the main bridge of Jinzhou Bridge, the measured data of the key sections of the main tower and main beam are tracked and analyzed under various critical conditions.

(1) The stress of the bridge tower

The comparison between the measured values and theoretical values of the stress on the left and right sides of section 7–7 of the tower during some key construction stages is shown in Fig. 19 and Fig. 20.

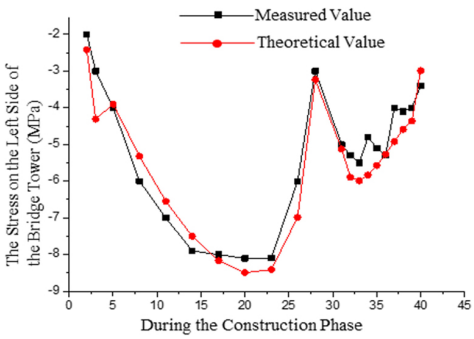

Fig. 19. Comparison chart between measured and theoretical stress values on the left side of the bridge tower during the construction phase

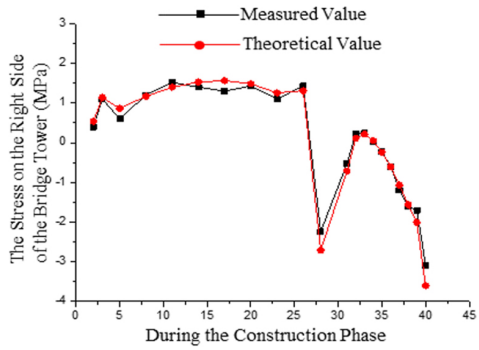

Fig. 20. Comparison chart between measured and theoretical stress values on the right side of the bridge tower during the construction phase

From the above chart, it can be inferred that in each construction phase, the measured stress values of the left and right sides of the bridge tower have small differences compared to the theoretical values. The trends are similar, and the stress levels of the sections are within the allowable range. This indicates that the structural load is safe and reasonable.

(2) Main beam

1. Stress of the main beam

Considering the monitoring section 1–1, located on the cast-in-place concrete main beam, the comparison between the measured stress values and theoretical values of the upper and lower edges at various construction stages is depicted in Fig. 21 and Fig. 21.

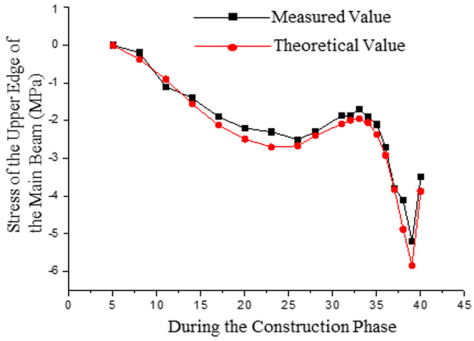

Fig. 21. Comparison of measured and theoretical stress values of the upper edge of the main beam during construction stages

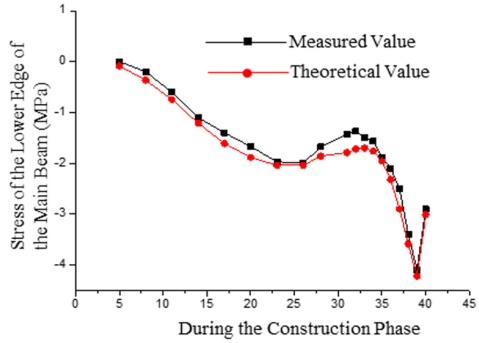

Fig. 22. Comparison chart between measured and theoretical stress values on the right side of the bridge tower during the construction phase

Based on the above chart, it can be observed that the measured and theoretical stress values of the upper and lower edges of the main beam during each construction stage exhibit small discrepancies and follow similar trends. The stresses across the sections are within the allowable range, indicating the structural integrity and safety of the load distribution.

2. Displacement of the main beam

Taking the node at the C6 cable-stayed position as a representative, the uplift displacement of the main beam during the construction process is shown in Fig. 23.

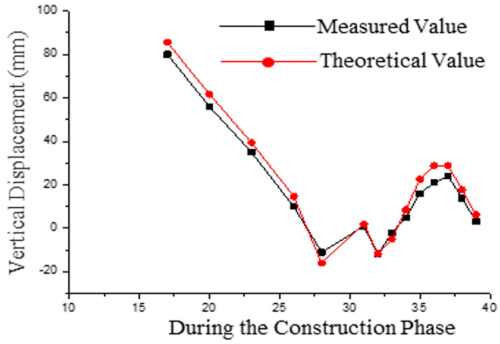

Fig. 23. The comparison between the measured uplift displacement values and theoretical values of the main beam in each construction phase

Based on the data shown in the graph, it can be observed that the measured uplift displacements of the main beam are consistently lower than the theoretical calculated values. This is because during the model establishment, it is not possible to simulate all the detailed structures inside the steel box girder, resulting in a decrease in the stiffness of the main beam and consequently reducing the measured displacements.

(3) Cable force testing

The tension force variation of cable C6 during the construction process is shown in Fig. 24 and Fig. 25.

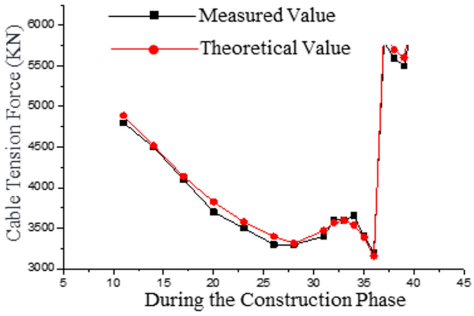

Fig. 24. The comparison between measured and theoretical values of the tension force on the south side of cable C6 in each construction stage

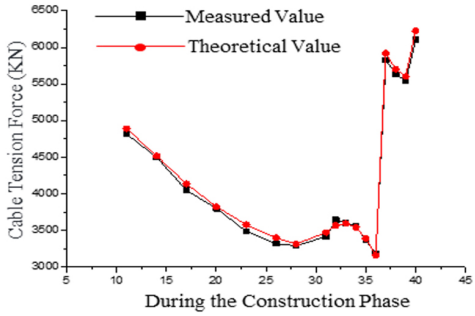

Fig. 25. The comparison between measured and theoretical values of the tension force on the north side of cable C6 in each construction stage

Based on the analysis of the above figure, it can be observed that the measured values and theoretical values of the tension force on cable C6 in each construction stage are almost identical, showing similar trends. The tension forces on the north and south sides of the cable differ only slightly, indicating a well-balanced force distribution and a favorable stress state of the inclined cable.

5.2. Effect of bridge state control

5.2.1. Elevation of the main beam

During the bridge erection, in order to compare with the design elevation, the measurement position of the main beam is the center of the asphalt layer on the bridge deck corresponding to the control elevation of each stage in the construction phase. The comparison between the as-erected curve and the design curve is shown in Fig. 26. The results indicate that the measured values of the bridge deck profile of Jinzhou Bridge's main span are in good agreement with the design elevation, with a relatively small relative error within ±20 (excluding the pre-camber value). The maximum error is 16, and the main beam profile is smooth.

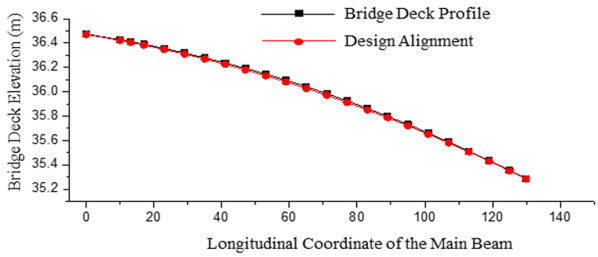

Fig. 26. Comparison graph of measured and designed values of bridge deck elevation in the completed bridge state

5.2.2. Cable tension

According to Table 2, the difference between the measured cable tension and the design tension, as well as the theoretical calculated tension, is very small in the bridge's completed state, with a relative error of less than ±3%. The difference in cable tension between the north and south sides of the bridge at the same position is very small, with a relative error of less than ±1.5%. The distribution of cable tension is reasonably balanced.

Table 2. Table of measured differences in cable tension between the north and south sides in the completed bridge state

Cable number	C1	C2	C3	C4	C5	C6	C7	C8	C9
The difference in cable tension between the north and south sides (kN)	−10.0	−60.2	−38.8	−17.7	−25.9	70.9	17.3	−20.1	−26.1
Design cable tension (kN)	6926	6572	6150	5810	5504	4922	4564	3724	3059
The difference in cable tension divided by the design cable tension (%)	−0.14	−0.92	−0.63	−0.30	−0.47	1.44	0.38	−0.54	−.85

5.2.3. Structural stress

According to the measurement results from the sensors, the stress variations of the main girder and bridge piers were calculated. The stress distribution results for the critical sections of the main girder and bridge piers in the completed bridge state are shown in Figs. 27–30.

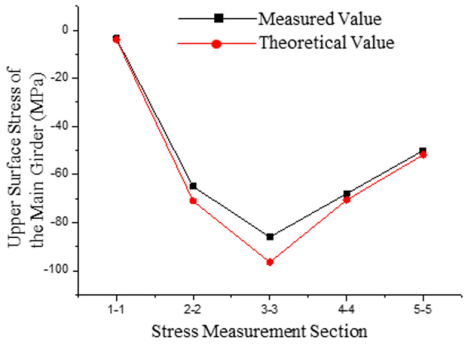

Fig. 27. Comparison graph of upper surface stresses of the main girder in the completed bridge state

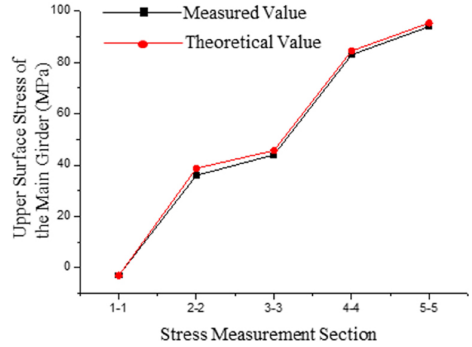

Fig. 28. Comparison graph of lower surface stresses of the main girder in the completed bridge state

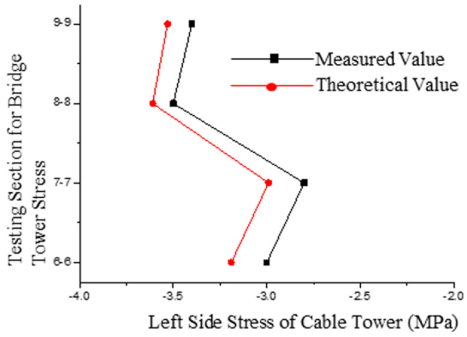

Fig. 29. Comparison graph of left side stresses of bridge towers in the completed bridge state

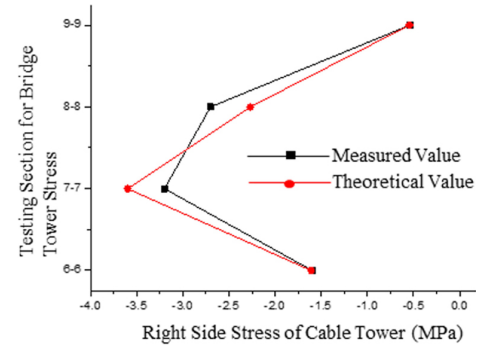

Fig. 30. Comparison graph of right side stresses of bridge towers in the completed bridge state

Based on the data in the above graph, it can be observed that the measured stresses of the main beam and the stress testing section of the bridge tower are in good agreement with the theoretical values. The numerical difference is minimal, indicating that the structural load state is safe and reliable. The theoretical analysis is accurate, and the control effect is satisfactory.

6. Conclusions

This article compares the measured values and theoretical values of structural internal forces and deformations in both the construction and completed states of the Jinzhou Bridge. It concludes that the main bridge of Jinzhou Bridge is structurally well-loaded and the

bridge structure is safe and reliable. The main beam's alignment is generally smooth, further confirming the accuracy of the construction control theory data.

- Construction state
  Under various working conditions, the measured stress on the upper and lower flanges of the key section of the main beam matches well with the theoretical values. The load-bearing condition of the main beam structure is good and complies with the design requirements, ensuring its safety and reliability.
  Regarding cable forces, the error in cable forces under different working conditions is controlled within ±2%, meeting the maximum allowable cable force deviation requirement in the design. The tensioning of the cables is reasonable, indicating proper cable force distribution.
- Under the completed state of the bridge
  Under the completed state of the bridge, the measured cable forces of the inclined cables show a small difference compared to the designed and theoretically calculated values, with a deviation of less than ±3%. The difference in cable forces between the north and south sides of the bridge at the same position is also small, with a relative error of less than ±1.5%. This indicates a reasonable distribution of cable forces and proper tensioning of the inclined cables.

References

[1] P. Nisha and Y. Turkan, "Bridge construction progress monitoring using lidar and 4D design models", *Automation in Construction*, vol. 109, art. no. 102961, 2020, doi: 10.1016/j.autcon.2019.102961.

[2] M. Pańtak, "Comparative analysis of dynamic load models generated by runners on footbridges", *Archives of Civil Engineering*, vol. 69, no. 1, pp. 147–162, 2023, doi: 10.24425/ace.2023.144165.

[3] H. Sousa, et al., "Design and implementation of a monitoring system applied to a long-span prestressed concrete bridge", *Structural Concrete*, vol. 12, no. 2, pp. 82–93, 2011, doi: 10.1002/suco.201000014.

[4] Z. Xianghong and Z. Binjiang, "Construction monitoring method of gui dan intercity bridge in guang zhou", *Applied Mechanics and Materials*, vol. 578, pp. 1157–1160, 2014, doi: 10.4028/www.scientific.net/AMM.578-579.1157.

[5] L. J. Butler, W. Lin, and J. Xu, "Monitoring, modeling, and assessment of a self-sensing railway bridge during construction", *Journal of Bridge Engineering*, vol. 23, no. 10, 2018, doi: 10.1061/(ASCE)BE.1943-5592.0001288.

[6] L. Chengyuan, H. Zhuowei, and L. Wei, "Study on temperature characteristics of multi-tower cable-stayed bridge", *Archives of Civil Engineering*, vol. 69, no. 4, pp. 535–548, 2023, doi: 10.24425/ace.2023.147675.

[7] M. M. Alamdari, et al., "Non-contact structural health monitoring of a cable-stayed bridge: Case study", *Structure and Infrastructure Engineering*, vol. 15, no. 8, pp. 1119–1136, 2019, doi: 10.1080/15732479.2019.1609529.

[8] Y. Ji, W. Liu, and W. Li, "Anti-overturning safety performance investigation for single column pier bridge", *Archives of Civil Engineering*, vol. 68, no. 3, pp. 221–240, 2022, doi: 10.24425/ace.2022.141882.

[9] T. C. Huynh, J. H. Park, and J. T. Kim, "Structural identification of cable-stayed bridge under back-to-back typhoons by wireless vibration monitoring", *Measurement*, vol. 88, pp. 385–401, 2016, doi: 10.1016/j.measurement.2016.03.032.

[10] V. Straupe and A. Paeglitis, "Analysis of geometrical and mechanical properties of cable-stayed bridge", *Procedia Engineering*, vol. 57, pp. 1086–1093, 2013, doi: 10.1016/j.proeng.2013.04.137.

[11] G. Hongye, et al., "Construction monitoring of self-anchored suspension bridge with inclined tower", *Journal of Bridge Engineering*, vol. 26, no. 10, 2021, doi: 10.1061/(ASCE)BE.1943-5592.0001777.

[12] H. Zhiguo, et al., "Integrated structural health monitoring in bridge engineering", *Automation in Construction*, vol. 136, art. no. 104168, 2022, doi: 10.1016/j.autcon.2022.104168.

[13] V. Racic and J. B. Morin, "Data-driven modelling of vertical dynamic excitation of bridges induced by people running", *Mechanical Systems and Signal Processing*, vol. 43, no. 1-2, pp. 153–170, 2014, doi: 10.1016/j.ymssp.2013.10.006.

[14] A. Vilventhan and R. Rajadurai, "4D bridge information modelling for management of bridge projects: a case study from India", *Built Environment Project and Asset Management*, vol. 10, no. 3, pp. 423–435, 2020, doi: 10.1108/BEPAM-05-2019-0045.

[15] T. Siwowski, H. Zobel, T. Al-Khafaji, and W. Karwowski, "FRP bridges in Poland: state of practice", *Archives of Civil Engineering*, vol. 67, no. 3, pp. 5–27, 2021, doi: 10.24425/ace.2021.138040

Received: 2023-12-28, Revised: 2024-03-19